Strong Coupling Between Plasmons and Molecular Excitons in Metal-Organic Frameworks

Alexander D. Sample,[1] Jun Guan,[2] Jingtian Hu,[1] Thaddeus Reese,[3] Jeong-Eun Park,[1] Francisco Freire-Fernández,[1] Charles Cherqui,[1] Richard D. Schaller,[1,4] George C. Schatz[1,2] and Teri W. Odom[1,2,3]*

[1]Department of Chemistry, [2]Graduate Program in Applied Physics, and [3]Department of Materials Science and Engineering, Northwestern University, Evanston, IL 60208; [4]Center for Nanoscale Materials, Argonne National Laboratory, Argonne, IL 60439

Abstract

This communication describes the strong coupling of plasmonic nanoparticle lattices to densely packed molecular emitters in metal-organic frameworks (MOFs). We realized strong coupling from porphyrin-derived emitters with small dipole moments by assembling these molecules as ligands into an ordered MOF film on arrays of Ag nanoparticles. Dispersion measurements of the lattice-MOF system revealed the formation of anti-crossing polariton bands, a signature feature of strong coupling. We also demonstrated controllable coupling strength through detuning of the plasmon energy by the surrounding solvents. Through transient absorption spectroscopy, we reveal that the lower polariton mode has a lifetime similar to the uncoupled MOF exciton while the upper polariton lifetime is >10 times longer and may favor intersystem crossing to a triplet state ($S_1 \rightarrow T_1$) instead of $S_1 \rightarrow S_0$ decay. This system shows the potential of MOFs as an excitonic material for future polariton chemistry research.

Keywords: *metal–organic framework, plasmonic nanoparticle array, conformal coating, surface lattice resonance, ultrafast spectroscopy*

TOC Graphic

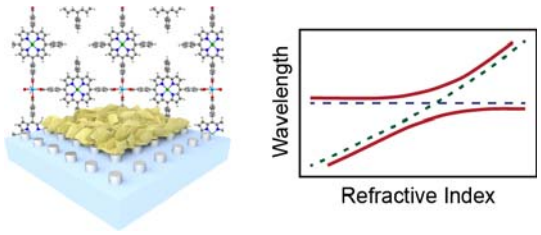

Metal-organic frameworks (MOFs) are porous, ordered materials consisting of metal nodes and organic ligands whose thin-film form is being integrated into optical devices.[1-3] Luminescent MOFs can be designed from emissive ligands, lanthanide metal nodes, host-guest interactions, or by loading pores with fluorescent molecules.[4-5] Critically, significantly higher concentrations of ligand-based emitters can be assembled within MOFs without aggregation-induced quenching compared to solution.[4-5] For example, surface-mounted MOF (SURMOF) films synthesized by a layer-by-layer method can support ~525 emitters into a 10^3 nm^3 volume, while only 0.3 emitters are possible in a saturated solution of the same volume.[6] Despite these advantages, MOFs often show lower photoluminescence (PL) intensity than organic dyes because ligands that are optimized for chemical stability typically lack the delocalized π systems and rigidity needed for high quantum yields.[7] PL efficiency of MOFs can be improved by reducing crystal defects or ligand design to limit nonradiative decay channels;[8] however, these approaches are often chemically incompatible with film growth processes.

Although the PL of MOFs can be improved by external stimuli such as solvent exchange and guest-host interactions,[9] these chemical approaches have limited influence. Photonic cavities show stronger effects and can increase PL intensity and as well as control the emission wavelength of MOFs.[10-11] Previously, we showed that cavities based on plasmonic nanoparticle (NP) lattices coupled with porphyrin SURMOFs resulted in 16-fold higher PL intensity and two-fold decrease in exciton lifetime compared to the pristine SURMOF.[6] These NP arrays support surface lattice resonances (SLRs), collective plasmonic-photonic modes whose wavelength can be easily tuned by changing the dielectric environment.[12-14]

Optical cavities and excitons can form hybridized polariton states in the strong coupling regime when the coupling strength (g) exceeds emitter and cavity losses.[15-17] Because $g \propto 2d\sqrt{\frac{\hbar\omega_0}{2\varepsilon_0}\frac{N}{V}}$,[18-

[19] strong coupling usually requires emitters with large transition dipole moments (d) and intense absorption bands. MOFs can concentrate emitters (to increase N/V) and align their dipole moment to optical fields over distances above 100 nm, which has facilitated polariton formation with Fabry-Perot cavities formed by two parallel mirrors.[10-11] Such closed architecture cavities rely on varying the incident light angle to detune the energy and are only semi-transparent, which limits the control of the cavity environment after fabrication. In contrast, the solvent and molecules surrounding open cavities such as NP lattices can be exchanged to allow continuous tuning of the coupling strength without changing the measurement conditions and can be utilized for applications in reactivity control[20] and sensing.[21]

Here we show that MOF films coupled to plasmonic NP lattices can generate exciton polaritons. We observed strong coupling between low transition-dipole-moment porphyrin ligands within a SURMOF and a Ag NP lattice with characteristic upper polariton (UP) and lower polariton (LP) modes. By changing the solvent within the MOF pores, we detuned the SLR energy across the MOF Q_1 and Q_2 exciton bands for continuous and reversible evolution between weak and strong coupling. Transient absorption spectroscopy measurements revealed that the LP amplitude-averaged lifetime was 4.8 ± 1.7 ps, which is faster than the uncoupled exciton and appears to follow a similar decay pathway. Interestingly, the UP lifetime was >10 times longer (168 ± 2 ps), which indicates that strong coupling opens new slower decay pathways not observed in uncoupled MOF excitons.

Figure 1 depicts the plasmonic NP lattice-MOF system for strong coupling. We selected a Pd-P MOF with a Zn paddlewheel node and a Pd-metalated porphyrin ligand (**Figure 1a**) to obtain a higher transition dipole moment d than the free base analogue.[6, 22] The Ag NP lattice (height h =

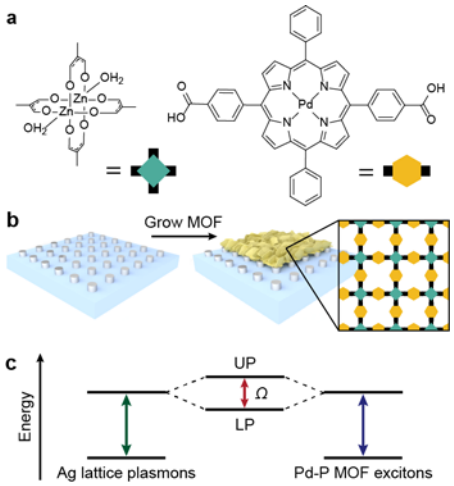

Figure 1: Overview of strongly coupled Ag NP lattice-Pd-P MOF system. (**a**) Metal node and organic linker of Pd-P MOF structure. (**b**) Depiction of Ag NPs covered with Pd-P MOF nanocrystal film (**c**) Schematic diagram of strong coupling between lattice plasmons and MOF excitons.

60 nm, diameter D = 70 nm, periodicity a_0 = 350 nm) on quartz was fabricated by the PEEL method[23-24] and designed to support an SLR mode isoenergetic with the Q_1 absorption band of the Pd-P MOF. Next, the Ag NPs were passivated with a thin layer of alumina and then treated with an oxygen plasma to facilitate the growth of a conformal SURMOF film (~60 nm) using layer-by-layer spray coating[6, 25] (**Figure 1b**). X-ray diffraction patterns and absorption spectra of the Pd-P MOF film are in good agreement with literature values (Figure S1).

We measured the photonic band structures from our NP lattice-MOF system by angle-resolved spectroscopy to compare the dispersive properties of the polariton modes to the pristine SURMOF and plasmonic NP lattice (**Figure 2**). As expected, the Q_1 absorption band of the Pd-P MOF is constant at 2.34 eV at all incident angles (**Figure 2a**). The bare Ag NP lattice has 2 sets of (0, ±1) diffraction modes[26] from the quartz substrate (n = 1.45) and the superstrate solvent (n = 1.40, shown with white lines), which highlights the sensitivity of the lattice to changes and differences in refractive index (**Figure 2b**). In contrast, the NP lattice-MOF system shows a lower polariton

(LP) mode with a signature anti-crossing behavior at ~60 meV below the Q_1 exciton energy in

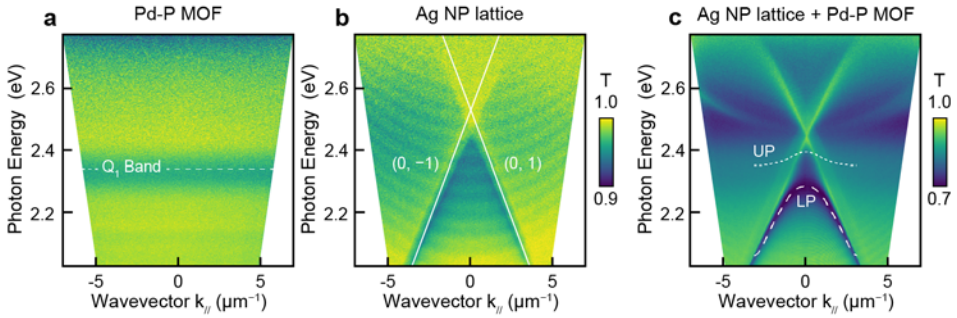

Figure 2: Modified dispersion properties are observed when Ag NP lattices are coupled to the Pd-P MOF film. Dispersion diagrams of (**a**) pristine Pd-P MOF film, (**b**) bare Ag NP lattice, and (**c**) coupled Ag NP + MOF system under TE polarization. The angle independent Q_1 band energy is indicated with dashed white line in (**a**), and the (0, ±1) diffractive orders are indicated with solid lines in (**b**). Modeling for upper and lower polariton bands are added for clarity. Diagrams were measured n=1.40 index solvents

addition to the (0, ±1) diffraction mode with the NP lattice (**Figure 2c**). The upper polariton (UP) has a relatively low transmission intensity and is not visible in the measurement (Figure S3) but can be predicted by modeling.[27-28] The calculated LP mode matches well with experiment result, and using the predicted UP position, we estimate a Rabi splitting of 110 meV (Figure S4). Because of negative detuning where the SLR is lower in energy than the Q_1 band, the LP mode has more plasmon character and therefore resembles the highly angle dependent energy of the uncoupled SLR mode. The predicted UP mode, however, is more exciton-like and is expected to be dispersive only when the magnitude of k is less than 2 μm^{-1}.

To determine the NP lattice-MOF interactions at different coupling strengths, we tuned the dielectric environment with solvents having different refractive indices. **Figure 3** depicts how the detuning of the SLR tailors coupling with MOF excitons. Coupling is maximized when the cavity mode and exciton energy are the same. In our system, the coupling is largest when the substrate index matches the effective superstrate index from both the MOF and the solvent n. By changing

the solvent (and the effective superstrate index) above n = 1.29, the SLR was negatively detuned

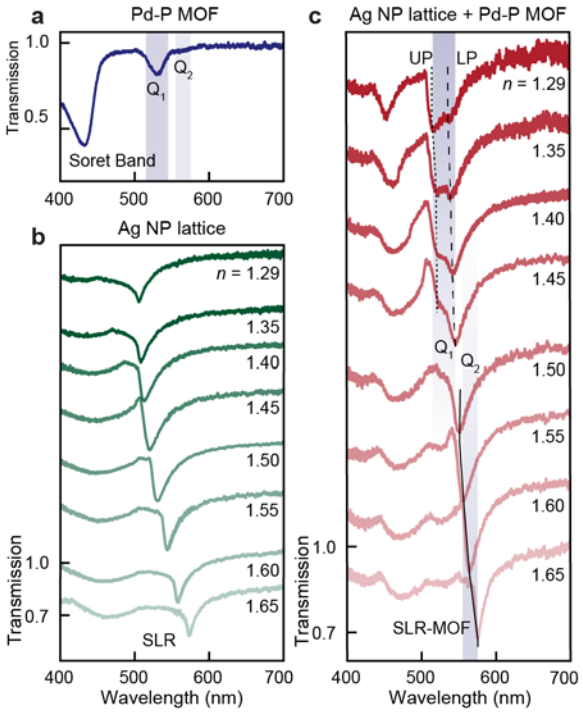

Figure 3: Detuning of SLR energy by refractive index superstrate shows tunable Rabi splitting. Transmission spectra at normal incidence of (**a**) bare Pd-P MOF film, (**b**) Ag NPs, and (**c**) MOF-covered Ag NPs. Bare MOF spectrum was taken with an n =1.40 index solvent. Ag NPs and Ag NPs + MOF spectra were taken with various index solvents (n = 1.29 − 1.65) and are offset by 0.25 for clarity. The FWHM of the MOF Q bands are shown in **a** and **c** with blue vertical bands. The MOF contribution to refractive index is not considered in the n values labeled in **c**.

from the Q_1 exciton, which increased the SLR character and transmission intensity of the LP. The pristine Pd-P SURMOF (**Figure 3a**) showed the Q_1 band at λ = 530 nm, the Q_2 band at λ = 564 nm, and the Soret band at λ = 440 nm. The quality and transmission intensity of the SLR mode could be changed by mismatching refractive index of the superstrate and solvent (**Figure 3b**); the mode wavelength was controllable from λ = 506 nm to 574 nm (with n = 1.29 and 1.65 solvents, respectively) and can therefore couple to either the Q_1 or Q_2 band of the Pd-P MOF. In **Figure 3c**, we changed the solvent index n to tune from strong coupling with the Q_1 band (dashed lines) to

weak coupling with the Q_2 band (solid line). The largest splitting between UP and LP minima (112 meV) was observed with n = 1.29, which is in good agreement with the predicted Rabi splitting in Figure 2c (110 meV). As n was increased to 1.45, the relative intensity of the UP decreased while the LP increased. With n = 1.50 – 1.65, the lineshape seems to resemble that of an SLR with a small modification from the Q_2 band, similar to what has been observed for a weakly coupled plasmon-modified exciton.[6] By varying n, we can continuously access different coupling strengths and a full transition from the strong to weak coupling regime.

We performed ultrafast transient absorption (TA) spectroscopy to determine how the decay dynamics of the strongly coupled system were different from the uncoupled components (**Figure 4**). In the pristine Pd-P SURMOF spectral map, the bleach signals at λ = 437 nm and 530 nm are from the Soret and Q_1 bands, respectively, and the dip in induced absorption at λ = 564 nm is from the Q_2 band (**Figure 4a**). When fit to a biexponential decay, the Q_1 band has an amplitude-averaged

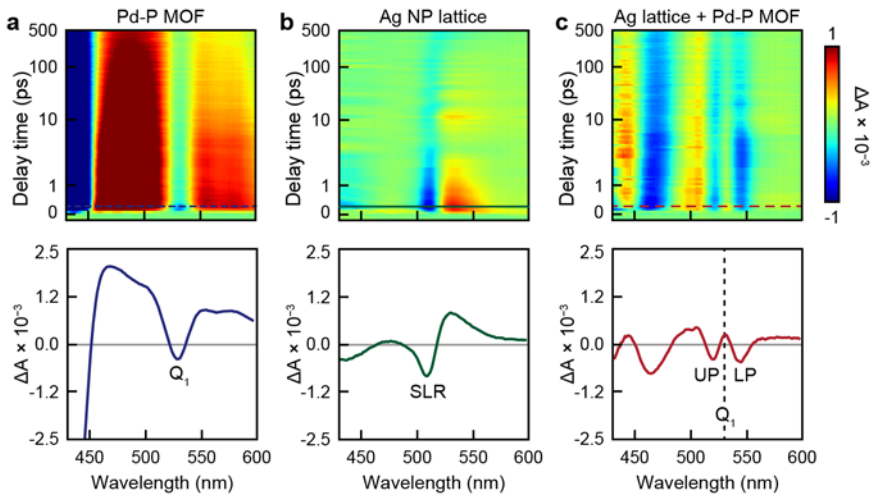

Figure 4: Two distinct transient absorption modes are observed in coupled system. (**a-c**) TA spectral maps (top) and OD signal cross sections at 300 fs (bottom) for (**a**) bare Ag lattice (**b**) pristine SURMOF and (**c**) coupled system. Vertical dashed line in (**c**) indicates position of uncoupled MOF Q_1 band. Samples were pumped at 400 nm with a fluence of 130 μJ/cm^2 in n = 1.40 refractive index environment. Broad bleach near 440 nm in (**a**) is from localized surface plasmon mode.

lifetime of 10.8 ± 0.1 ps (Table S1), which is similar to other porphyrin MOF films.[6, 29] The t_1 lifetime of the Q_1 band is 0.3 ± 0.0 ps from vibrational relaxation, and the t_2 lifetime of 61.9 ± 8.5 ps is the decay from $S_1 \rightarrow S_0$. The intersystem crossing ($S_1 \rightarrow T_1$) of the Pd-P SURMOF characterized by a long lifetime (>100 μs)[22] was not observed because of triplet state quenching by oxygen in ambient conditions.[30] Ag NP lattices showed two bleach signals from photoinduced absorption: (1) a strong bleach signal at λ = 510 nm at the SLR wavelength, and (2) a weaker bleach at λ = 430 nm at the localized surface plasmon wavelength of the individual NPs (**Figure 4b**). Using a single-exponential model, we determined that the SLR mode has an amplitude-averaged lifetime of 1.1 ± 0.1 ps (Table S2), which is consistent with the expected timescales of electron-phonon scattering.[6, 31]

In the strongly coupled system (**Figure 4c**), the bleach signals appear at the wavelengths of the UP and LP and show lifetimes that are distinct from each other and their uncoupled components. The polariton modes are separated by 105 meV, which is an excellent agreement with the model and spectral measurements. The amplitude-averaged LP and UP lifetimes (4.8 ± 1.7 ps and 168 ± 2 ps) can be fit to a bi-exponential (Table S3-4) but are not directly determined from the lifetimes of the uncoupled states as is the case in the weak coupling regime.[6, 32] The averaged LP lifetime is faster than lifetime of Pd-P SURMOF and slower than the uncoupled SLR, which is consistent with other strong coupling systems.[19] Interestingly, the averaged UP lifetime is an order of magnitude longer than the exciton, which indicates that the UP decay pathways are slower than that of the uncoupled components. The UP fast decay component (t_1 = 0.3 ± 0.1 ps) is comparable to the pristine MOF, but the slow decay component (t_2 = 572.7 ± 62.0 ps) is much longer than the conventional $S_1 \rightarrow S_0$ relaxation and approaches timescales for intersystem crossing (>100 ps). Because the pristine Pd-P MOF does not show this longer decay component, the UP may create a

new decay pathway where intersystem crossing becomes favorable even in the presence of oxygen. Manipulation of triplet decay channels has been demonstrated in other organic molecule-based polariton systems[33-35] and therefore should be possible in this system.

In summary, we demonstrated strong coupling between a porphyrin-based MOF and Ag NP lattice. Signature anti-crossing behavior was observed in the dispersion diagram with two polariton modes with hybrid dispersion properties. The NP lattice-MOF system also showed Rabi splitting in the transmission spectra that can be tuned by shifting the SLR wavelength with different refractive index solvents that fill the MOF pores. Ultrafast measurements revealed that the lifetime of the LP is faster than the uncoupled exciton while the UP is an order of magnitude larger, which suggests that new energy pathways are possible from this hybridized mode. We anticipate that these results will serve as a new platform for continuously tunable plasmon-exciton coupling with precise control over coupling strength and polariton properties. With advancements in luminescent MOF materials and thin film growth techniques, we predict that strong coupling phenomena such as low threshold lasing and Bose-Einstein condensation will be possible in NP lattice-MOF systems.

Acknowledgements.

This work was supported by the Vannevar Bush Faculty Fellowship from the U.S. Department of Defense (DOD N00014-17-1-3023). CC and GCS (theory) were funded by the Department of Energy, Office of Basic Energy Sciences under grant DE-SC0004752. This work made use of the NUFAB, EPIC, and SPID facilities of Northwestern University's NUANCE Center and the Jerome B.Cohen X-Ray Diffraction Facility, which have received support from the SHyNE Resource

(NSF ECCS-2025633), the IIN, and Northwestern's MRSEC Program (NSF DMR-1720139). This work also made use of the Pritzker Nanofabrication Facility, which receives partial support from the SHyNE Resource, a node of the NSF National Nanotechnology Coordinated Infrastructure (NSF ECCS-2025633). Use of the Center for Nanoscale Materials, an Office of Science user facility, was supported by the U.S. Department of Energy, Office of Science, Office of Basic Energy Sciences, under Contract No. DE-AC02-06CH11357. The authors thank Dr. Stephen A. Miller and the Northwestern University Laser and Electronics Design Core Facility for assistance on instrumentation.

Supporting Information Available:

The Supporting Information is available free of charge at XXX

- Materials, fabrication and measurement information, x-ray diffraction data, modeling details, additional transient absorption and angle-resolved measurements, transient absorption decay fitting

REFERENCES

1. Stavila, V.; Talin, A. A.; Allendorf, M. D., MOF-based electronic and opto-electronic devices. *Chemical Society Reviews* **2014,** *43* (16), 5994-6010.
2. Haldar, R.; Heinke, L.; Wöll, C., Advanced Photoresponsive Materials Using the Metal–Organic Framework Approach. *Advanced Materials n/a* (n/a), 1905227.
3. Medishetty, R.; Zareba, J. K.; Mayer, D.; Samoc, M.; Fischer, R. A., Nonlinear optical properties, upconversion and lasing in metal-organic frameworks. *Chemical Society Reviews* **2017,** *46* (16), 4976-5004.
4. Cui, Y.; Yue, Y.; Qian, G.; Chen, B., Luminescent Functional Metal–Organic Frameworks. *Chemical Reviews* **2012,** *112* (2), 1126-1162.
5. Allendorf, M. D.; Bauer, C. A.; Bhakta, R. K.; Houk, R. J. T., Luminescent metal–organic frameworks. *Chemical Society Reviews* **2009,** *38* (5), 1330-1352.
6. Liu, J.; Wang, W.; Wang, D.; Hu, J.; Ding, W.; Schaller, R. D.; Schatz, G. C.; Odom, T. W., Spatially defined molecular emitters coupled to plasmonic nanoparticle arrays. *Proceedings of the National Academy of Sciences* **2019,** *116* (13), 5925-5930.
7. Liu, X.-Y.; Lustig, W. P.; Li, J., Functionalizing Luminescent Metal–Organic Frameworks for Enhanced Photoluminescence. *ACS Energy Letters* **2020,** *5* (8), 2671-2680.
8. Wei, Z.; Gu, Z.-Y.; Arvapally, R. K.; Chen, Y.-P.; McDougald, R. N.; Ivy, J. F.; Yakovenko, A. A.; Feng, D.; Omary, M. A.; Zhou, H.-C., Rigidifying Fluorescent Linkers by Metal–Organic Framework Formation for Fluorescence Blue Shift and Quantum Yield Enhancement. *Journal of the American Chemical Society* **2014,** *136* (23), 8269-8276.
9. Lustig, W. P.; Mukherjee, S.; Rudd, N. D.; Desai, A. V.; Li, J.; Ghosh, S. K., Metal–organic frameworks: functional luminescent and photonic materials for sensing applications. *Chemical Society Reviews* **2017,** *46* (11), 3242-3285.
10. Haldar, R.; Fu, Z.; Joseph, R.; Herrero, D.; Martín-Gomis, L.; Richards, B. S.; Howard, I. A.; Sastre-Santos, A.; Wöll, C., Guest-responsive polaritons in a porous framework: chromophoric sponges in optical QED cavities. *Chemical Science* **2020,** *11* (30), 7972-7978.
11. Kottilil, D.; Gupta, M.; Tomar, K.; Zhou, F.; Vijayan, C.; Bharadwaj, P. K.; Ji, W., Cost-Effective Realization of Multimode Exciton–Polaritons in Single-Crystalline Microplates of a Layered Metal–Organic Framework. *ACS Applied Materials & Interfaces* **2019,** *11* (7), 7288-7295.
12. Zou, S.; Janel, N.; Schatz, G. C., Silver nanoparticle array structures that produce remarkably narrow plasmon lineshapes. *The Journal of Chemical Physics* **2004,** *120* (23), 10871-10875.
13. Yang, A.; Hoang, T. B.; Dridi, M.; Deeb, C.; Mikkelsen, M. H.; Schatz, G. C.; Odom, T. W., Real-time tunable lasing from plasmonic nanocavity arrays. *Nature Communications* **2015,** *6*, 6939.
14. Wang, W.; Ramezani, M.; Väkeväinen, A. I.; Törmä, P.; Rivas, J. G.; Odom, T. W., The rich photonic world of plasmonic nanoparticle arrays. *Materials Today* **2018,** *21* (3), 303-314.
15. Frisk Kockum, A.; Miranowicz, A.; De Liberato, S.; Savasta, S.; Nori, F., Ultrastrong coupling between light and matter. *Nature Reviews Physics* **2019,** *1* (1), 19-40.
16. Väkeväinen, A. I.; Moerland, R. J.; Rekola, H. T.; Eskelinen, A. P.; Martikainen, J. P.; Kim, D. H.; Törmä, P., Plasmonic Surface Lattice Resonances at the Strong Coupling Regime. *Nano Letters* **2014,** *14* (4), 1721-1727.

17. Dovzhenko, D. S.; Ryabchuk, S. V.; Rakovich, Y. P.; Nabiev, I. R., Light–matter interaction in the strong coupling regime: configurations, conditions, and applications. *Nanoscale* **2018,** *10* (8), 3589-3605.
18. Wu, Y.; Yang, X., Strong-Coupling Theory of Periodically Driven Two-Level Systems. *Physical Review Letters* **2007,** *98* (1), 013601.
19. Wang, H.; Wang, H.-Y.; Sun, H.-B.; Cerea, A.; Toma, A.; De Angelis, F.; Jin, X.; Razzari, L.; Cojoc, D.; Catone, D.; Huang, F.; Proietti Zaccaria, R., Dynamics of Strongly Coupled Hybrid States by Transient Absorption Spectroscopy. *Advanced Functional Materials* **2018,** *28* (48), 1801761.
20. Thomas, A.; Lethuillier-Karl, L.; Nagarajan, K.; Vergauwe, R. M. A.; George, J.; Chervy, T.; Shalabney, A.; Devaux, E.; Genet, C.; Moran, J.; Ebbesen, T. W., Tilting a ground-state reactivity landscape by vibrational strong coupling. *Science* **2019,** *363* (6427), 615-619.
21. Yoshihara, F.; Fuse, T.; Ashhab, S.; Kakuyanagi, K.; Saito, S.; Semba, K., Superconducting qubit–oscillator circuit beyond the ultrastrong-coupling regime. *Nature Physics* **2017,** *13* (1), 44-47.
22. Adams, M.; Kozlowska, M.; Baroni, N.; Oldenburg, M.; Ma, R.; Busko, D.; Turshatov, A.; Emandi, G.; Senge, M. O.; Haldar, R.; Wöll, C.; Nienhaus, G. U.; Richards, B. S.; Howard, I. A., Highly efficient 1D triplet exciton transport in a palladium-porphyrin based surface-anchored metal-organic framework. *ACS Applied Materials & Interfaces* **2019**.
23. Henzie, J.; Lee, M. H.; Odom, T. W., Multiscale patterning of plasmonic metamaterials. *Nature Nanotechnology* **2007,** *2*, 549.
24. Lee, M. H.; Huntington, M. D.; Zhou, W.; Yang, J.-C.; Odom, T. W., Programmable Soft Lithography: Solvent-Assisted Nanoscale Embossing. *Nano Letters* **2011,** *11* (2), 311-315.
25. Arslan, H. K.; Shekhah, O.; Wohlgemuth, J.; Franzreb, M.; Fischer, R. A.; Wöll, C., High‐Throughput Fabrication of Uniform and Homogenous MOF Coatings. *Advanced Functional Materials* **2011,** *21* (22), 4228-4231.
26. Guo, R.; Hakala, T. K.; Törmä, P., Geometry dependence of surface lattice resonances in plasmonic nanoparticle arrays. *Physical Review B* **2017,** *95* (15), 155423.
27. Cherqui, C.; Bourgeois, M. R.; Wang, D.; Schatz, G. C., Plasmonic Surface Lattice Resonances: Theory and Computation. *Accounts of Chemical Research* **2019,** *52* (9), 2548-2558.
28. Yadav, R. K.; Bourgeois, M. R.; Cherqui, C.; Juarez, X. G.; Wang, W.; Odom, T. W.; Schatz, G. C.; Basu, J. K., Room Temperature Weak-to-Strong Coupling and the Emergence of Collective Emission from Quantum Dots Coupled to Plasmonic Arrays. *ACS Nano* **2020,** *14* (6), 7347-7357.
29. Gu, C.; Zhang, H.; Yu, J.; Shen, Q.; Luo, G.; Chen, X.; Xue, P.; Wang, Z.; Hu, J., Assembled Exciton Dynamics in Porphyrin Metal–Organic Framework Nanofilms. *Nano Letters* **2021,** *21* (2), 1102-1107.
30. Gijzeman, O. L. J.; Kaufman, F.; Porter, G., Oxygen quenching of aromatic triplet states in solution. Part 1. *Journal of the Chemical Society, Faraday Transactions 2: Molecular and Chemical Physics* **1973,** *69* (0), 708-720.
31. Hodak, J. H.; Martini, I.; Hartland, G. V., Spectroscopy and Dynamics of Nanometer-Sized Noble Metal Particles. *The Journal of Physical Chemistry B* **1998,** *102* (36), 6958-6967.
32. Canaguier-Durand, A.; Genet, C.; Lambrecht, A.; Ebbesen, T. W.; Reynaud, S., Non-Markovian polariton dynamics in organic strong coupling. *The European Physical Journal D* **2015,** *69* (1), 24.

33. Berghuis, A. M.; Halpin, A.; Le-Van, Q.; Ramezani, M.; Wang, S.; Murai, S.; Gómez Rivas, J., Enhanced Delayed Fluorescence in Tetracene Crystals by Strong Light-Matter Coupling. *Advanced Functional Materials* **2019,** *29* (36), 1901317.
34. Polak, D.; Jayaprakash, R.; Lyons, T. P.; Martínez-Martínez, L. Á.; Leventis, A.; Fallon, K. J.; Coulthard, H.; Bossanyi, D. G.; Georgiou, K.; Petty, I. I. A. J.; Anthony, J.; Bronstein, H.; Yuen-Zhou, J.; Tartakovskii, A. I.; Clark, J.; Musser, A. J., Manipulating molecules with strong coupling: harvesting triplet excitons in organic exciton microcavities. *Chemical Science* **2020,** *11* (2), 343-354.
35. Stranius, K.; Hertzog, M.; Börjesson, K., Selective manipulation of electronically excited states through strong light–matter interactions. *Nature Communications* **2018,** *9* (1), 2273.